IN-SITU CHARACTERIZATION OF PHASE TRANSFORMATIONS AND MICROSTRUCTURE EVOLUTION IN A γ-TiAl BASED ALLOY

Klaus-Dieter Liss[1], Arno Bartels[2], Helmut Clemens[3], Andreas Stark[2], Thomas Buslaps[4], Dominic Phelan[5], LaReine A. Yeoh[1]

[1] Bragg Institute, Australian Nuclear Science and Technology Organisation, Private Mail Bag 1, Menai, NSW 2234, Australia; E-mail: liss@kdliss.de, kdl@ansto.gov.au
[2] Institute of Materials Science and Technology, Hamburg University of Technology, Eissendorferstrasse 40, D-21073 Hamburg,Germany
[3] Department of Physical Metallurgy and Materials Testing, Montanuniversität, Franz-Josef-Strasse 18, A-8700 Leoben, Austria
[4] European Synchrotron Radiation Facility B. P. 220, F-38043 Grenoble Cedex, France
[5] Engineering Materials Institute / Faculty of Engineering, University of Wollongong, Northfield Avenue, Wollongong NSW 2500, Australia

Abstract

Phase diagrams and microstructures of titanium aluminides are rather complex and, so far, little data were observed in-situ at elevated temperatures. We report on two-dimensional high energy X-ray diffraction and complementary laser scanning confocal microscopy to characterize the appearing phases and to follow the phase evolution in-situ and in real time.

As an example, the microstructure evolution of a quenched γ-TiAl alloy, consisting of α_2-Ti$_3$Al grains at room temperature, has been followed in both reciprocal and direct space as a function of temperature up to 1400 °C. At 700 – 800 °C extremely fine γ-laths are formed in α_2-grains occurring through an oriented rearrangement of atoms. Streaks linking reflections of both phases testify from coherent lattice and orientation gradients in the transforming crystallite. At temperatures around the eutectoid temperature recrystallization effects and the γ→α phase transition take place leading to grain refinement.

Introduction

Materials of light weight for the transportation and aerospace industries are of highest economical interest to reduce energy consumption during operation of the vehicle. Here γ-based titanium aluminides bear a high potential for applications in the medium temperature range to replace the double as dense nickel based superalloys [1]. The phase diagram [2] and the multitude of possible microstructures are rather complicated and may vary considerably between manufacturing temperatures of about 1300 °C and application temperatures of up to 800 °C. Usually, metallurgical investigations of the high temperature state take place under quenched conditions which are not only very time consuming and therefore coarse, but also assume a full understanding of the quench process itself. Modern characterization tools, however, such as synchrotron [3] and neutron [4] radiation or laser scanning confocal microscopy [5, 6] allow to acquire data in-situ and in real time during a thermo-mechanical simulation process. Here we

report on novel in-situ time resolved 2D diffraction and microscopy measurements which were conducted at elevated temperatures [7, 8, 9, 10]. The transition from α_2-Ti_3Al to γ-TiAl has been followed in both reciprocal and real space and is found to appear homogeneously over the bulk and to occur through an oriented rearrangement of atoms. At higher temperatures, the transition reverses and starts to grow slowly and stepwise from the grain boundaries into irregular shapes which impinge each other leading to grain refinement.

High Energy X-ray diffraction

High Energy X-rays or HEX-rays are very hard X-rays, with a photon energy between 80 keV and 1000 keV with practical interest around 100 keV and lie typically one order of magnitude higher in energy than conventional X-rays. They are produced on dedicated beamlines at modern synchrotron radiation sources. The main benefit is their deep penetration into matter which makes them a probe for bulk samples in materials science and facilitates sample environment and operation in air. Scattering angles are small and diffraction directed forward allowing for simple detector set-ups. Further, high momentum transfers Q can be reached for the study of liquid and amorphous materials. A review of this radiation and its applications has been given elsewhere by some of the authors [3].

Experimental data has been obtained from the beamlines id15a and id15b of the European Synchrotron Radiation Facility (ESRF). The white beam from the wiggler was monochromatized to about 100 keV (k = 50.6 Å⁻¹, λ = 0.124 Å) or 90 keV (k = 45.6 Å⁻¹, λ = 0.138 Å), respectively by a focusing silicon crystal and impinges the sample. A two-dimensional, flat detector out of a pool of i) a MAR345 online image plate, ii) an image intensifier coupled to a FReLoN CCD camera or iii) a Thales-Pixium 4700 flat panel pixel detector was placed behind the sample in order to record diffraction patterns in form of Debye-Scherrer rings.
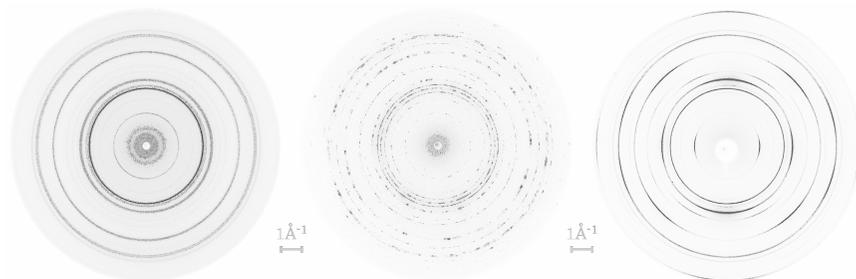
Figure 1: Different aspects of Debye Scherrer rings as obtained with high-energy X-rays from γ-TiAl material. Fine grained (left), coarse grained (middle) and textured (right) microstructure lead to different illumination of the rings

Typical Debye-Scherrer rings on titanium aluminides are presented in Figure (1). Simple relations between reciprocal lattice units $Q = 2\pi / d$, with lattice spacing d, and the radius R of a Debye-Scherrer ring exist for a well aligned detector normal to the incident beam: $Q = 2 k \sin(\theta)$ with Bragg angle $\theta = \frac{1}{2} atan(R / D)$, distance between sample and detector D and wave number $k = 2\pi / \lambda$. These formulas allow to reduce the two-dimensional (2D) rings into 1D patterns by azimuthal integration. A software package called dataRring has been written [11] and implemented using the SCILAB engine with the C language extension. It allows to determine automatically the center of a reasonable defined Debye Scherrer pattern, which can then be

further refined by a fitting process. The whole package is fully scriptable in order to process multiple diffraction patterns which can range up to several thousands for an in-situ data acquisition. Output files of dataRring are suitable for input to the Rietveld programs GSAS [12] with ExpGui [13] and MAUD [14], which reveal beyond others phase fractions, atomic order and disorder such as in the α_2-Ti$_3$Al phase or lattice parameters and their evolution [10].

Important aspects of the Debye Scherrer rings are also their 2D morphology, which may reveal fine grain, coarse grain or texture in the material, see Figure (1). The beam size is typical of 0.1×0.1 mm^2 and with a typical sample thickness of 4 mm defines an illuminated volume, from which crystallites can scatter. The number of crystallites in this volume being high for fine grained material, good orientation average and statistics occurs to illuminate continuously the whole Debye Scherrer rings. On the other hand, only a few crystallites are diffracting in coarse grained materials leading to a spotty pattern of discontinuous rings. In a (fine grained) textured sample, intensity at any one position around a given Debye Scherrer ring is proportional to the number of crystallites diffracting into this direction and therefore gives information about preferred orientation. An almost complete pole figure is then covered by taking multiple diffraction patterns upon full rotation of the sample around an axis perpendicular to the incident beam. dataRring allows to sector the ring patterns which is needed to sort the information into a pole figure [3].

In-situ diffraction experiments

High energy X-ray diffraction at modern synchrotron sources is very well suited for in-situ studies such as under elevated temperature or mechanical load. The beam intensity, the ease of setup and the time resolution of the detector allow to record patterns in steps of minutes (MAR345 image plate) down to fractions of a second (Thales Pixium and CCD detectors).

We have run titanium aluminide samples on temperature ramps from room temperature to 1400 °C. A cylindrical furnace with openings for the X-ray beams was used with an input of helium flow to reduce oxidation of the sample. Special care was taken for the sample mount which consisted of a hollow alumina stick and a collar of inner Ø 4 mm at its top end to hold a cylindrical sample of same diameter and of 10 mm height sitting in direct contact with the incorporated thermocouple of type-S. The α-rich sample has been ramped with 10 K / min to 1400 °C.

In-situ optical microscopy

A laser scanning confocal microscope has been set up with a high-temperature stage at the University of Wollongong [5, 6, 15, 16]. The focal distance of such a device is large enough to obtain images from inside a mirror-furnace which can operate up to 1800 °C. Further the narrow band-width and the scanning procedure through a pin-hole allow one to discriminate the signal from the thermal irradiation of the sample. The frame rate of the device is 30 s^{-1}.

α-Rich titanium aluminide

Initial specimens of α-rich Ti - 45Al - 7.5Nb (concentration in atomic %) material were prepared by tempering raw bulk material for 5 min at 1320 °C or 1335 °C and subsequently oil quenched in order to produce samples of reproducible microstructure resulting in 90 vol. % α_2-Ti$_3$Al and 10 vol. % massively transformed γ-TiAl phases in globular grains. Such a condition is far off the thermodynamical equilibrium and will evolve upon heating during an in-situ experiment to transform parts of the α_2-phase into γ-phase ($\alpha_2 \rightarrow \gamma$) until it reaches the eutectoid temperature

$T_{eu} = 1160\ °C$ at which α_2 disorders into α-phase ($\alpha_2 \to \alpha$) according to the phase diagram [2]. Above T_{eu}, the transformation ($\gamma \to \alpha$) takes place up to the α-transus at $T_\alpha = 1292\ °C$ (literature values from [17]). Since α is just the disordered phase of α_2, we work with a constant unit cell throughout the manuscript and mark all corresponding Miller indices in the α_2 notation.

Experimental results and discussion

The α-rich TiAl sample has been subjected to a heating cycle while diffraction patterns were taken in-situ with the image intensifier and coupled CCD camera about every 22 s. The intensity values of the reduced 1D powder diffraction patterns are depicted in gray scale in every line on the vertical time axis in figure (2). The temperature was raised by 10 K/min and the profile is overlaid to the right in the figure. Since temperature reading was affected by a linear offset it was calibrated to the α-transus temperature of $T_\alpha = 1292\ °C$ as obtained by differential scanning calorimetry measurements [17].
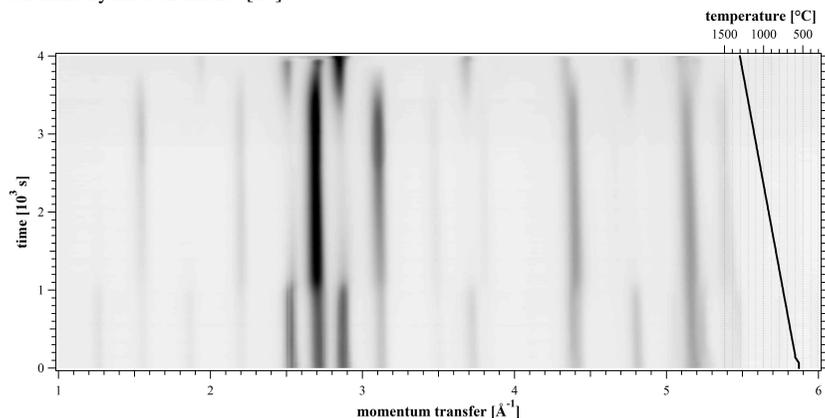
Figure 2: Gray scaled powder diffraction patterns (horizontal axis) evolving in time (vertical axis) on an imposed temperature ramp (top axis and overlaid graph) extracted from 2D ring patterns.

The most intense rings are the α-002 (using α_2 indexing) and the γ-111 reflections appearing superimposed at $G = 2.7\ Å^{-1}$. These fundamental reflections where all atoms scatter in phase (wave-mechanics) correspond to the nearly closed packed stacking sequences in the two phases (material) which also defines the well known Blackburn orientation relationship in the Ti-Al system. Adjacent are two α-rings namely α-200 at 2.5 $Å^{-1}$ and α-201 at 2.9 $Å^{-1}$, while the γ-200/002 pair appears together at 3.1 $Å^{-1}$. As one can see, the intensities evolve as a function of time. The integrated raw intensities of the four mentioned peaks are plotted in Figure (3). Little evolution is observed at lower temperatures while the α-phase starts to decrease in favor for γ-phase above 700 °C. While the γ-002/200 evolve continuously, the strongest γ-peak, γ-111 increases rapidly. However, very high peak intensities may be handled with caution due to saturation effects of the detector. The maximum of γ-material is reached at the eutectoid temperature and indeed, the peak of the γ-111 reflections coincides with the literature value of $T_{eu} = 1160\ °C$ [17]. The amount of α-phase increases again in cost of γ-phase until the latter vanishes at $T_\alpha = 1292\ °C$. Dynamics and grain growth in the α-field above are most rapid

leading to grain coarsening and therefore bad grain statistics and thus unrepresentative intensities.
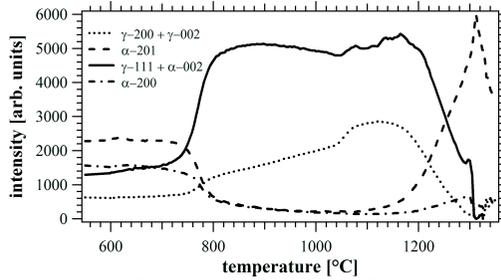
Figure 3: Intensity evolution of some characteristic reflections, extracted from figure (2).

Extracts of fully recorded Debye Scherrer rings are shown in Figure (4) for selected time frames from which the 1D information as discussed above had been obtained. Accordingly, a sample of identical starting conditions has been run in the laser scanning confocal microscope recording an in-situ movie from which extracted time frames are shown in Figure (5). Below 700 °C, the polished surface remains smooth and does sparely reveal any features (5a). The diffraction patterns do not yet differ substantially from that obtained beforehand at room temperature: Randomly distributed Bragg reflections lie on barely occupied Debye-Scherrer rings testifying a relatively large grain size in comparison to the beam size.

At increasing temperatures ultrafine lamellar microstructures appear homogeneously all over the bulk of the α_2-grains and can be resolved in the microscope, which further evolve to what is shown in Figure (5c) at 850 °C. Note, that some smaller grains do not transform at all, consisting already of massively transformed γ-phase. In reciprocal space, streaks evolve, Figure (4b) starting around an existing α_2-201 reflection and extending along a well defined direction. When these streaks cross the position of the γ-002/200 ring, intensity accumulates there. A movie created in real time from a sequence of experimental snapshots from the detector shows, that the intensity is shuffled along the streak until the α_2-phase fades away leaving behind bright γ-reflections, see Figure (4b-g). The streaks extend a fair way through reciprocal space and sometimes link several reflections of both phases on a straight line, which testifies to the high order and orientation relationship in the transforming region of the grain. The angular spread at given radius in Q-space is intrinsically narrow, so there is no mosaic spread evolving from incoherency in this complex structure. Further, reflections as the shoulder near a-201 in Figure (4c,d,e) occur from neither of the two phases and thus revealing an intermediate structure.

The phase diagram and the intensity studies from Figure (3) accordingly reveal, that the reverse transformation ($\gamma \rightarrow \alpha$) takes place above the eutectoid temperature, at which point the amount of γ-phase is maximal. The micrograph taken at 1100 °C shows indeed some new features which nucleate and develop at the grain boundaries. They evolve stepwise in a highly irregular shape as displayed for 1250 °C and their contrast becomes sharper until the α-transus is reached.

 Features in the surface relief as observed by the microscope will remain once they were created and thus are still visible above the phase transitions, Figure (5e), although we know from other studies, that the system has already transformed into pure α. In reciprocal space, the correlated α-reflection regains some intensity (4h), which occurs by the reverse transformation in the bulk of the lamellar colonies, before almost all streaks disappear (4i) and the morphology, particularly of the α-rings changes to a less spiky but more continuous distribution stemming from a finer grain size (4j-l). Yet the remaining matrix breaks up and the formerly sharp γ-reflections widen

their mosaic spread up to 10°. Even the massively transformed material is now affected by this transition and shows a very fine grained evolution of its microstructure.
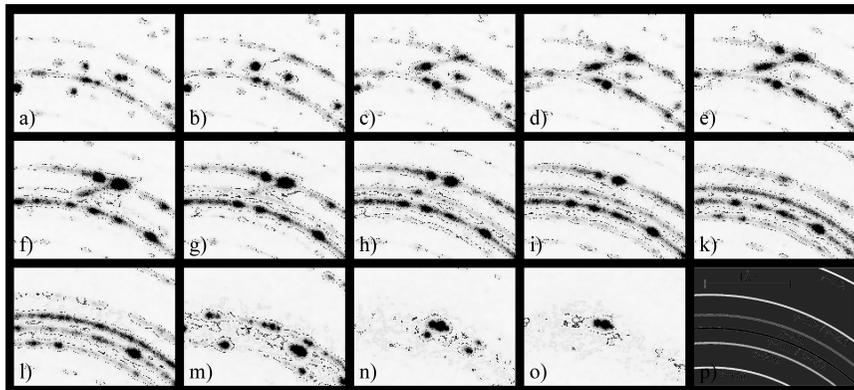
Figure 4: Diffraction pattern from the α-rich TiAl sample evolving qualitatively on a temperature ramp (10 K/min), registered at ID15A with the image intensifier and the CCD camera. Sections of Debye Scherrer rings are shown with a common center well below each image. A legend is given in p) indexing from inside out γ-110, α-200, γ-111 and α-002 coinciding, α-201 and the almost unresolved doublet γ-002 / γ-200. Initially large α-grains and few γ-spots a) exist; a faint streak forms around α-201 and γ-002 b); which evolves in c), forming an opposite shoulder d) and extends to α-002 / γ-111 e). The γ-002 / γ-200 intensity takes over in f) and the α-201 peak almost fades away g) when the transformation reverses for a short time to feed intensity back h). The streak disappears completely i) and grain refinement occurs k) to l). Above the α-transus m), no γ-rings are left and grain growth occurs rapidly until o). The 1D data in Figure (2) were reduced from these data.

Streaks in reciprocal space may occur on various occasions, such as gradients, truncation rods and diffuse scattering from phonons and here we may observe a superposition of all. Truncation rods, i.e. the peak broadening from the finite thickness of the lamellae play a role at the beginning of the phase transition, when extremely fine lamellae in the order of nanometers in thickness form. Next, the streaks take over a large fraction of intensity, which is comparable with the reflections of the pure phases, such that a considerable amount of the material must exist in gradual transition states. The streaks are vectorial revealing both a well defined and correlated radial and an angular or transverse component, expressed by a narrow but long streak. This gives evidence, that a continuous distribution of lattice parameters exists, each linked through a well defined orientation angle to the original lattice orientation. Intermediate states exist in which the new lattice parameter grows gradually and coherently while the lattice mismatch is caught by continuous, small angle grain boundaries.

Another process, discontinuous coarsening [18], is starting at the lamellar colony boundaries at temperatures above 1000 °C. The boundaries migrate into neighbouring colonies leaving behind coarser $(\alpha_2+\gamma)$ lamellae (Figure 5d,e). The phase composition of this newly formed lamellae is almost ideal, thus leading to the additional increase of γ-phase which can be observed in this temperature range in Figure (3). Moreover, the higher, almost fcc symmetry of the γ-phase gives raise to 4 possible orientations of the nucleating, almost hcp α_2-phase, in the coarsened lamellae. Above T_e the now existing surplus γ-phase has to transform back to α-phase (γ→α). One

mechanism may just reverse as observed in a short reverse flux along the faint streak in reciprocal space which transforms the central bulk of the colonies (4h). Secondly, the recrystallized laths at the colony boundaries transform and grow into the bulk of the colonies. Again, the crystallographic relationship between α and γ allows 4 possible α orientations after the transformation, which finally impinge to each other and lead the observed grain refinement in the diffraction pattern (Figure 4j-l).
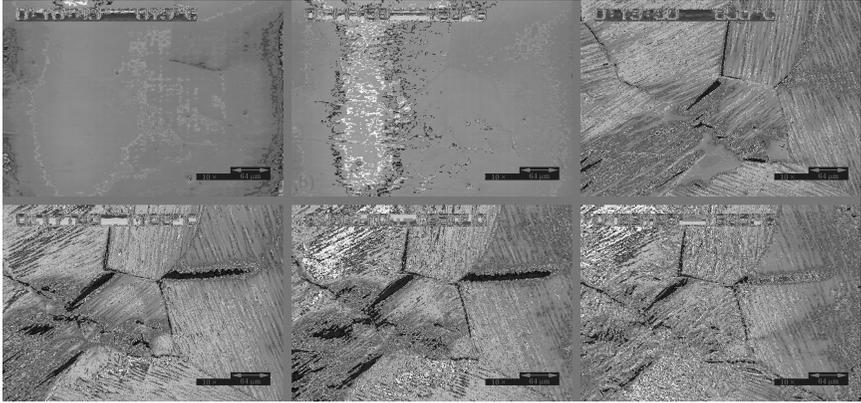
Figure 5 Micrographs obtained by laser confocal scanning microscopy from the α-rich TiAl sample at selected temperatures which evolve in time as shown in the annotations. The heating ramp was about 25 K/min.

Conclusion

High energy X-rays are excellent in-situ characterization tools with extreme potential of development for data analysis and applications. The real time in-situ laser scanning confocal microscopy method complements the diffraction results in order to obtain unprecedented understanding of the evolution of phases and microstructure. Here we demonstrated for the first time the return into thermo-dynamic equilibrium of a quenched, α-rich TiAl alloy. The phase evolution starts suddenly at about 700 °C by a creation of an ultrafine lamellar structure all over the α-grains. Transcendent states lead to intermediate reflections and directed lattice parameter gradients, testifying a high degree of coherency in this transition. Above the eutectoid temperature, the thermodynamic equilibrium shifts towards a higher amount of α-phase, such that the previously created γ-phase has to transform back again. However, the Blackburn relation allows four equivalent orientations of α-phase to grow on a γ-lattice, leading to grain refinement observed in the diffraction pattern.

Acknowledgement

Reference list

[1] H. Kestler, H. Clemens, "Titanium and Titanium Alloys", WILEY-VCH (2003) p. 351-392

[2] J. C. Schuster, M. Palm: "Reassessment of the Binary Aluminum-Titanium Phase Diagram", Journal of Phase Equilibria and Diffusion 27 (2006) p. 255-277

[3] K.-D. Liss, A. Bartels, A. Schreyer, H. Clemens: "High energy X-rays: A tool for advanced bulk investigations in materials science and physics", Textures and Microstructures 35-3/4 (2003) p. 219-252

[4] D. P. Riley, C. P. Oliver, E. H. Kisi: "In-Situ Neutron Diffraction of Titanium Silicide, Ti5si3, During Self-Propagating High-Temperature Synthesis (SHS)", Intermetallics 14 (2006) p. 33-38

[5] D. Phelan, R. Dippenaar: "Widmannstätten Ferrite Plate Formation in Low-Carbon Steels", Metallurgical and Materials Transactions A 35 (2004) p. 3701-3706

[6] D. Phelan, M. Reid, N. Stanford, R. Dippenaar: "In-Situ Observations of Phase Transformations in Titanium", JOM 58 (2006) p. 67-69

[7] K.-D. Liss, A. Bartels, H. Clemens, S. Bystrzanowski, A. Stark, T. Buslaps, F.-P. Schimansky, R. Gerling, C. Scheu, A. Schreyer: "Recrystallization and phase transitions in a γ-TiAl based alloy as observed by ex- and in-situ high-energy X-ray diffraction", Acta Materialia 54-14 (2006) p. 3721-3735

[8] K.-D. Liss, H. Clemens, A. Bartels, A. Stark, T. Buslaps: "Phase Transitions and Recrystallization in a Ti-46at%Al-9at%Nb Alloy as Observed by In- Situ High-Energy X-ray Diffraction", Advanced Intermetallic-Based Alloys - Mater. Res. Soc. Symp. Proc. 0980, Warrandale, PA (2007) p. II05-07

[9] K.-D. Liss, A. Bartels, H. Clemens, S. Bystrzanowski, A. Stark, T. Buslaps, F.-P. Schimansky, R. Gerling, A. Schreyer: "A study of recrystallization and phase transitions in intermetallic titanium aluminides by in-situ high-energy X-Ray diffraction", Materials Science Forum 539-543 (2007) p. 1519-1524

[10] L. A. Yeoh, K.-D. Liss, A. Bartels, H. F. Chladil, M. Avdeev, H. Clemens, R. Gerling, T. Buslaps: "In-Situ High Energy X-Ray Diffraction Study and Quantitative Phase Analysis in the α+γ Phase Field of Titanium Aluminides", Scripta Materialia 57 (2007) p. 1145-1148

[11] LaReine Yeoh, Klaus-Dieter Liss. "dataRring". Lucas Heights, Australia, Bragg Institute, ANSTO (2006)

[12] A. C. Larson, R. B. Von Dreele: "Anonymous General Structure Analysis System (GSAS)". LAUR 86-748. Los Alamos National Laboratory. (2000)

[13] B. H. Toby: "Expgui, a Graphical User Interface for GSAS", Journal of Applied Crystallography 34 (2001) p. 210-213

[14] L. Lutterotti: "Quantitative Rietveld analysis in batch mode with Maud, and new features in Maud 2.037", IUCR CPD Newsletter 32 (2005) p. 53-55

[15] D. Phelan, N. Stanford, R. Dippenaar: "In Situ Observations of Widmanstatten Ferrite Formation in a Low-Carbon Steel", Materials Science and Engineering A - Structural Materials Properties Microstructure and Processing 407 (2005) p. 127-134

[16] D. Phelan, M. Reid, R. Dippenaar: "Kinetics of the Peritectic Phase Transformation: In-Situ Measurements and Phase Field Modeling", Metallurgical and Materials Transactions A - Physical Metallurgy and Materials Science 37A (2006) p. 985-994

[17] H. F. Chladil, H. Clemens, G. A. Zickler, M. Takeyama, E. Kozeschnik, A. Bartels, T. Buslaps, R. Gerling, S. Kremmer, L. A. Yeoh, K.-D. Liss: "Experimental studies and thermodynamic simulation of phase transitions in high Nb containing γ-TiAl based alloys", International Journal of Materials (Zeitschrift für Metallkunde) 98 (2007) p. 1131-1137

[18] S. Mitao, L. A. Bendersky: "Morphology and growth kinetics of discontinuous coarsening in fully lamellar Ti-44 Al (at.%) alloy", Acta Materialia 45-11 (1997) p. 4475-4489